Supporting information

Hierarchical structure LiFePO₄@C synthesized by oleylamine-mediated method for low temperature applications

Jingmin Fan, Jiajia Chen, Yongxiang Chen, Haihong Huang, Zhikai Wei, Ming-sen Zheng*, Quanfeng Dong*

Department of Chemistry, College of Chemistry and Chemical Engineering, Xiamen University, State Key Laboratory of Physical Chemistry of Solid Surfaces, Xiamen, Fujian, 361005, P. R. China

Synthesis of nano-LiFePO₄@C.

The nano-LiFePO₄@C was prepared by using the modified pure oleylamine route[1] followed by a carbonization procedure. In a typical synthesis of LiFePO₄@C, $FeCl_2$ (8 mmol) and $CH_3COOLi\ 2H_2O$ (8 mmol) were separately dissolved in 20 mL anhydrous ethanol. The two ethanol solutions and 1 mL aniline were added quickly into a continuously stirring 250 mL three-neck flask which was filled with 50 ml oleylamine at 100°C under nitrogen atmosphere, kept stirring at 100°C for 30 min. The solution color changed to brown. Then an H_3PO_4 (0.55 mL, ≥85%) anhydrous ethanol (5 mL) solution was also added dropwise into the reactor, the solution was then kept heating at 100°C for 1 h. Subsequently, the solution was heated from 100°C to 200°C within 40 min, and maintained 4 hours at 200°C, then cooled down to room temperature. The solution color changed to dark black. The resulted LiFePO₄ nanocrystals were precipitated by adding 30 mL of ethanol and collected by centrifugation at 6000 rpm, then they were washed by cyclohexane and ethanol for 2 times. Finally, the product dried at 65°C in a vacuum oven overnight. The resulting material was carbonized for 4 hours at 600°C at the rate of 5°C min⁻¹ under argon containing 5% H_2.

Characterizations

The synthesis products were characterized by powder X-ray diffraction (XRD), scanning electron microscopy (SEM), transmission electron microscopy (TEM), Raman spectroscopy and elemental analysis. The powder X-ray diffraction (XRD) measurements were performed with an X'pert PRO instrument (PANalytical) using Cu Kα radiation (λ = 0.15418 nm). TEM (including high-resolution transmission electron microscope, HRTEM) studies were performed on a TECNAI F-30 high-resolution transmission electron microscope operating at 300 kV. The samples were prepared by dropping ethanol dispersion of samples onto 300-mesh carbon-coated

copper grids and immediately evaporating the solvent. Scanning electron microscopy (SEM) was performed on scanning electron microscopes (Hitachi S-4800). Raman spectra were collected by a Ramshaw Raman microscope with an Ar laser 514 nm. Elemental analysis was performed on Vario EL III.

Electrochemical Measurements[2]

The electrochemical properties of the $LiFePO_4$@C were measured in CR2016 coin-type cells. The cells were formed using a Li metal negative electrode, a Celgrade polypropylene separator, an electrolyte of 1 M $LiPF_6$ in a 1:1:1 (volume) ethylene carbonate (EC), dimethyl carbonate (DMC), ethyl methyl carbonate (EMC) mixture. The cells were assembled in an argon-atmosphere-filled glove box, and then the cell was parepared by casting. To fabricate the positive electrode, a slurry of $LiMPO_4$ powders (80 wt%), carbon black (Super P, 10 wt%), 10 wt% water soluble polymer n-lauryl acrylate (LA, Chengdu, China) with a little water-ethanol dispersant were ball milling for 6 h, and painted on an aluminum substrate, then dried in vacuum at 65^oC overnight. The cells were galvanostatically charged and discharged with a Neware BT5-5V5mA Tester (Neware Co., Ltd, Shenzhen, China) at a voltage range of 2.4–4.2 V at room temperature. For $LiFePO_4$@C low temperature test, we run 0.1 C (17 mA g^{-1}) for two cycles at room temperature. Then the cells was put into a cryogenic insulation refrigeration box, the cells were charged and discharged at 2.4–4.2 V for 0^oC and 2.2–4.2 V for below 0^oC under certain rate of current. And all the charge and discharge capacities are based on the weight of $LiFePO_4$. At room temperature, 1 C = 170 mA g^{-1}, 1 C=140 mA g^{-1} for low temperature test. Cyclic voltammetry (CV) experiments were conducted using a Princeton PAR273A potentiostat at scan rates of 0.1mV s^{-1}. Electrochemical impedance measurements were carried out using a Zahner IM6 electrochemical workstation with an applied perturbation signal of 5 mV over the frequency range of 100 kHz to 10 mHz.
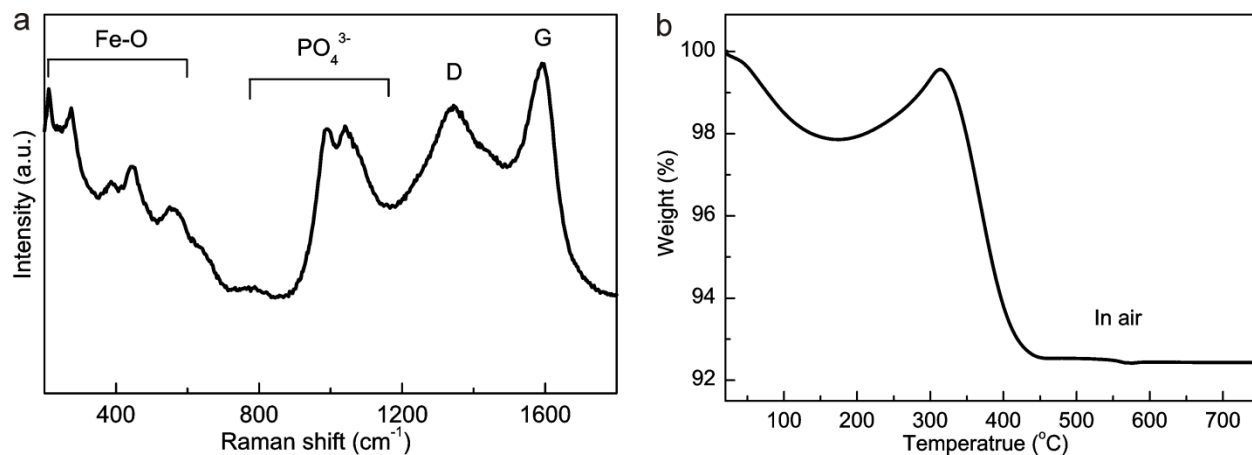
Figure S1. (a) Raman spectrum of the nano-LiFePO$_4$@C nanocomposite. The fundamental D and G bands of carbon occur at 1345 cm^{-1} and 1594 cm^{-1}. (b) Thermogravimetric analysis (TGA) curve of nano LiFePO$_4$@C.
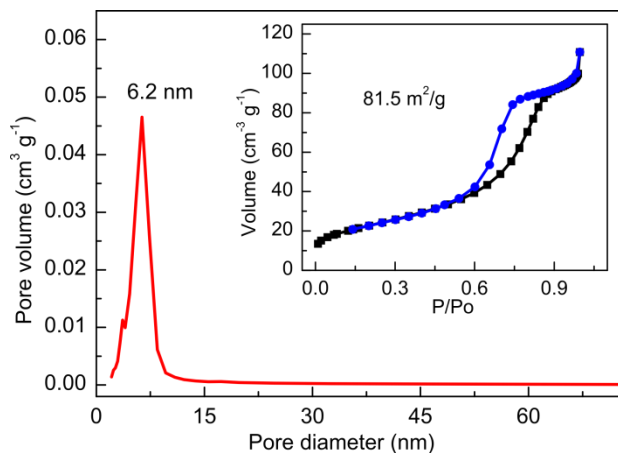
Figure S2. A desorption isotherm was used to determine the pore size distribution by the Barret–Joyner–Halender (BJH) method, the inset shows the corresponding nitrogen adsorption-desorption isotherms at 77 K.
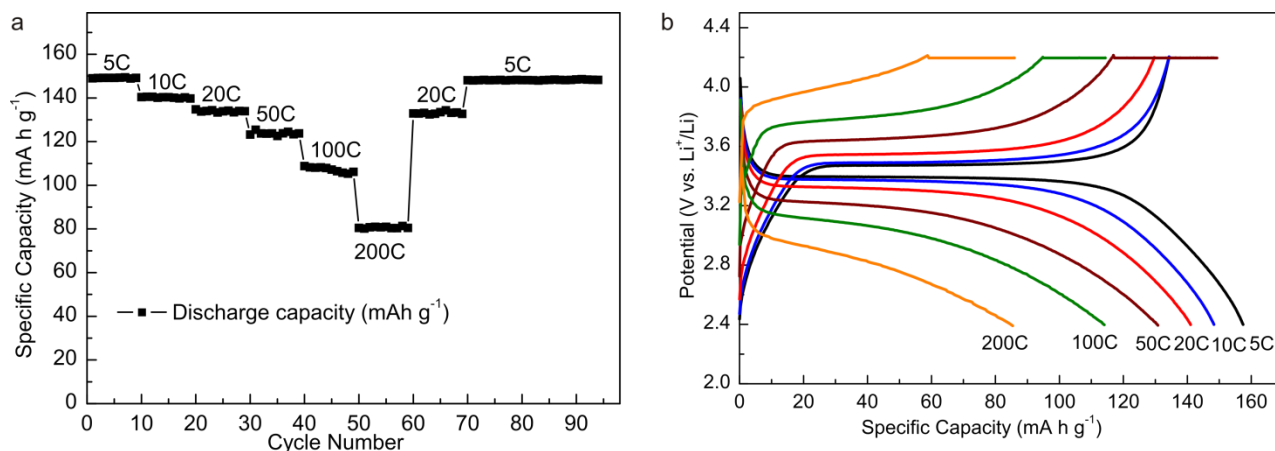
Figure S3. (a) Discharge capacity versus cycle number plots of LiFePO$_4$@C from 5C to 200C at room temperature. (b) corresponding charge/discharge curve of nano-LiFePO$_4$@C.
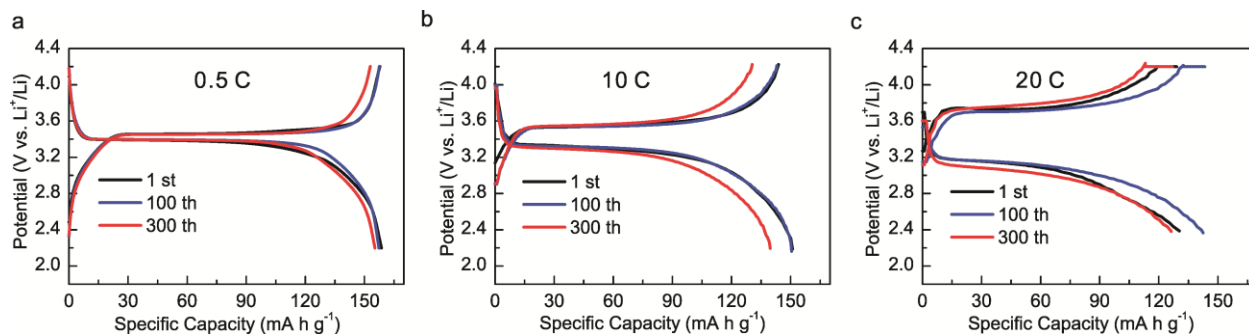
Figure S4. Charge/discharge curve at (a) 0.5C, (b) 10C, (c) 20C, respectively . 1C=170 mA g^{-1}.
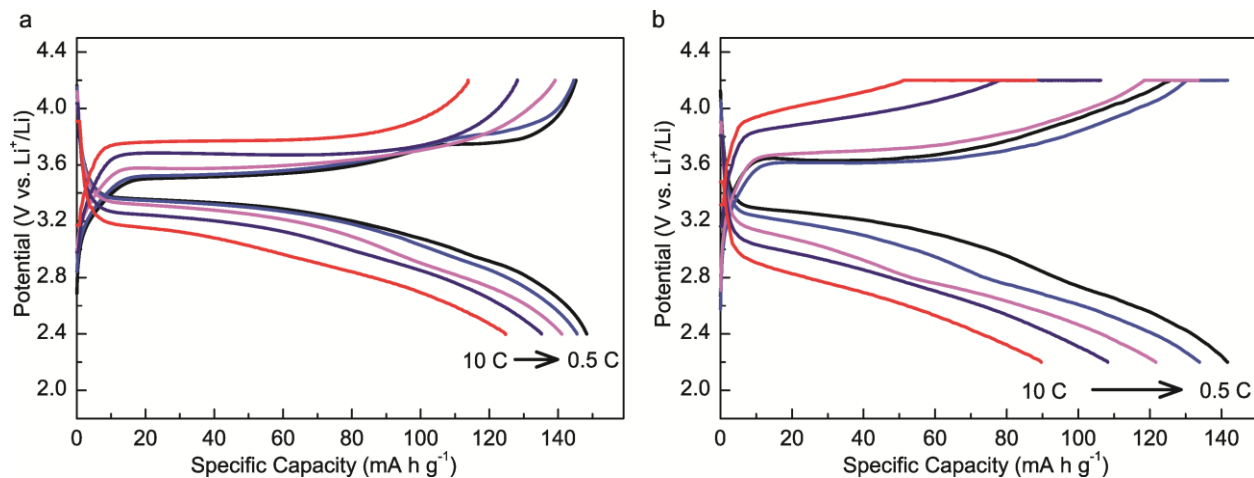
Figure S5. Charge/discharge curve of nano-LiFePO$_4$@C at (a) 0°C and (b) -20°C, respectively. 1C=140 mA g^{-1}.
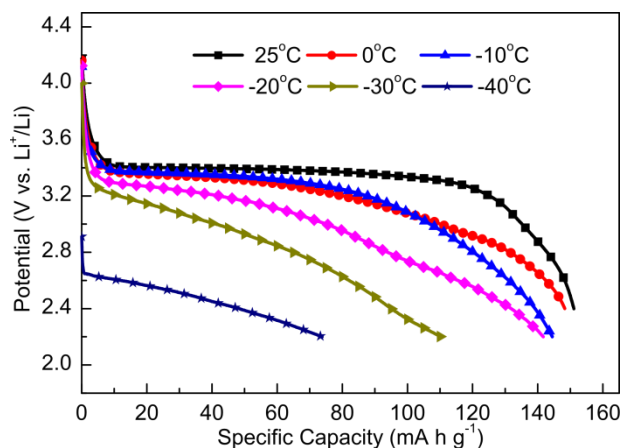
Figure S6. Discharge curve of nano-LiFePO$_4$@C in the temperature range of -40°C~25°C at discharge rate of 0.5C. Due to the nanosize effect and the electrical polarization at low temperature,[3, 4] the discharge curve of nano-LiFePO$_4$@C at 0.5C do not exhibit a well flat plateau especially below -20°C.
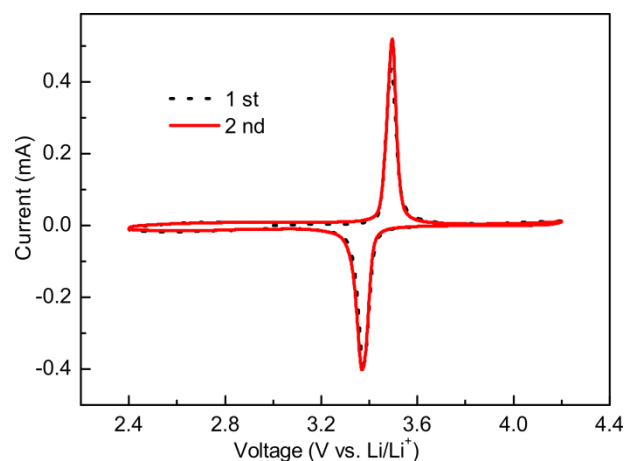
Figure S7. Cyclic voltammograms at a sweep rate of 0.1 mV s^{-1}.
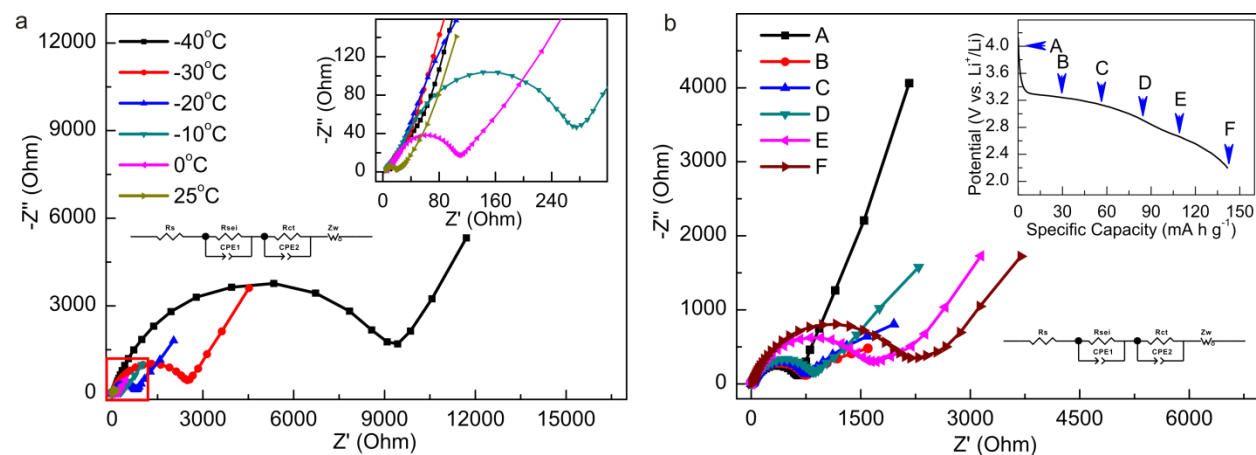
Figure S8. The typical Nyquist plots: (a) nano-LiFePO$_4$@C from 25°C to -40°C at full charge state. Inset of (a): enlarged profiles. (b) nano-LiFePO$_4$@C at different discharge state at -20°C. Inset of (b): showing the discharge curve for impedance measurements at 0.5C.

Table S1. Comparison of LiFePO$_4$/C reported in literatures

Materials	Morphology	size	Room temperature /mAh g^{-1}			Low temperature /mAh g^{-1}		Electrode formulation	Carbon content
			5 C	10C	100 C	-15 °C	-20 °C		
LiFePO$_4$ /C[5]	micro hollow spheres	~1 um	125	117	—	—	—	70:20:10	7.7 wt%
LiFePO$_4$ @C/CNT[6]	Nearly sphere	90 nm	—	128 (15C)	100	128 (0.2C)	—	85:10:5	5.7 wt%
LiFePO$_4$/C[7]	Nanosheets	Thickness: 4.3 nm	—	139	70 (80 C)	—	—	80:10:10	2 wt%
LiFePO$_4$/C[8]	Nanowire	Diameter: 100 nm	114	93	—	—	—	70:20:10	1 wt%
LiFePO$_4$/C[9]	nanoplate microspheres	Diameter:1-2 um	85		—	—	—	78:12:10	3.01 wt%
LiFePO$_4$/C/ppy[10]	Flowerlike microspheres	2-5 um	110	86	—	—	—	75:20:5	5 wt% ppy: 12 wt%
PEDOT-LiFePO$_4$[11]	Particles	200 nm	—	123	—	—	—	84.5:8:7.5	0
LiFePO$_4$/C[12]	Mesoporous nanocomposite	—	130	118	—	—	—	80:10:10	13 wt%
Double-coated carbon LiFePO$_4$[13]	Microspheres nanoporous	Primary particle 200-300 nm	—	115.6	—	—	75 (1C)	85:7.5:7.5	3.1 wt%
LiFePO$_4$/C[14]	—	—	95	—	—	—	90 (1C)	75:15:10	2.7 wt%
LiFePO$_4$/C[15]	—	—	110	—	—	—	78 (1C)	80:15:5	5 wt%
This work	Hierarchical microparticles	Primary particle 30 nm	149	140	107	—	133 (1 C)	80:10:10	6.7 wt%
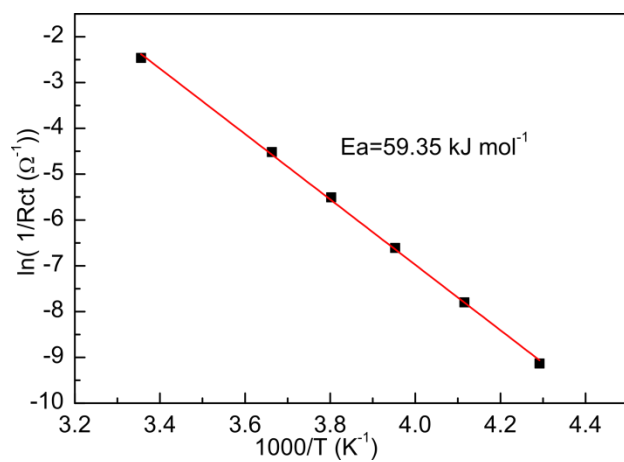
Figure S9. The linear relationship between 1000/T and ln(1/Rct).
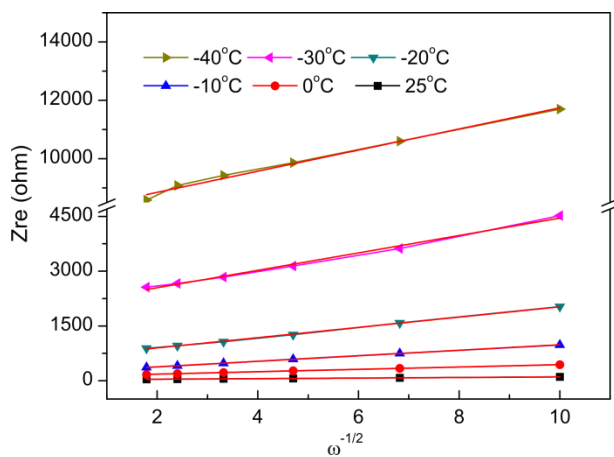
Figure S10. variations and fi ttings between Z re and the reciprocal square root of the angular frequency in the lowfrequency region of nano-LiFePO$_4$@C.
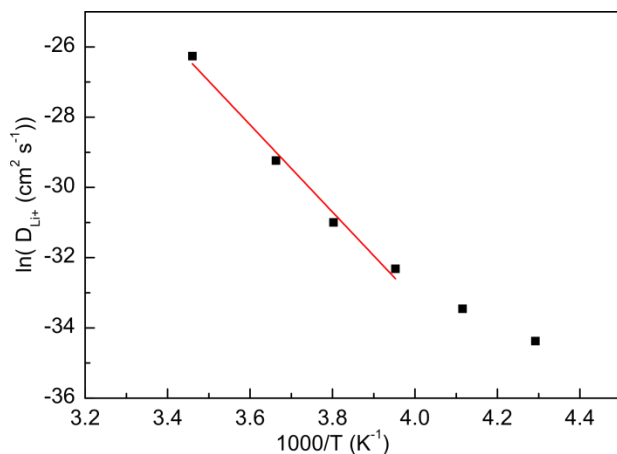
Figure S11. Arrhenius plots of the apparent chemical diffusion coefficient of lithium ions.

Table S2. Impedance parameters derived using equivalent circuit model and lithium diffusion coefficient D_{Li+} for nano-LiFePO$_4$@C.

Temperature	Rs (ohm)	Rsei (ohm)	Rct (ohm)	D_{Li+} $(cm^2 s^{-1})$
25°C	3.782	2.392	11.73	3.93×10^{-12}
0°C	5.399	6.825	91.46	2.01×10^{-13}
-10°C	4.057	13.21	245.9	3.45×10^{-14}
-20°C	4.562	19.58	742.9	9.23×10^{-15}
-30°C	5.815	30.12	2438	2.96×10^{-15}
-40°C	8.829	50.89	9258	1.18×10^{-15}

The diffusion coefficients D_{Li+} at various temperature are calculated based the Warburg region by using the following equation[16]:

$$D = (R^2T^2)/(2A^2n^4F^4C^2\sigma^2) \qquad (1)$$

Where R is the gas constant, T is the absolute temperature, A is the surface area of the cathode, n the number of electrons per molecule during oxidization, F the Faraday constant, C the concentration of lithium-ion (7.69×10^{-3} mol cm^{-3}), and σ is the Warburg factor associated with Zre (Zre$\propto\sigma\omega^{-1/2}$, as shown in Figure S10).

References

1. V. Mazumder and S. Sun, *J. Am. Chem. Soc.*, 2009, **131**, 4588-4589.

2. C. Wang, J. J. Chen, Y. N. Shi, M. S. Zheng and Q. F. Dong, *Electrochimica Acta*, 2010, **55**, 7010-7015.

3. G. Kobayashi, S. I. Nishimura, M. S. Park, R. Kanno, M. Yashima, T. Ida and A. Yamada, *Adv Funct Mater*, 2009, **19**, 395-403.

4. X. H. Rui, Y. Jin, X. Y. Feng, L. C. Zhang and C. H. Chen, *J. Power Sources*, 2011, **196**, 2109-2114.

5. S. Yang, M. Hu, L. Xi, R. Ma, Y. Dong and C. Y. Chung, *ACS Applied Materials & Interfaces*, 2013, **5**, 8961-8967.

6. X.-L. Wu, Y.-G. Guo, J. Su, J.-W. Xiong, Y.-L. Zhang and L.-J. Wan, *Adv. Energy Mater.*, 2013, **3**, 1155-1160.

7. X. Rui, X. Zhao, Z. Lu, H. Tan, D. Sim, H. H. Hng, R. Yazami, T. M. Lim and Q. Yan, *ACS Nano*, 2013, **7**, 5637-5646.

8. C. B. Zhu, Y. Yu, L. Gu, K. Weichert and J. Maier, *Angewandte Chemie-International Edition*, 2011, **50**, 6278-6282.

9. Y. M. Wu, Z. H. Wen and J. H. Li, *Advanced Materials*, 2011, **23**, 1126-1129.

10. C. W. Sun, S. Rajasekhara, J. B. Goodenough and F. Zhou, *Journal of the American Chemical Society*, 2011, **133**, 2132-2135.

11. D. Lepage, C. Michot, G. X. Liang, M. Gauthier and S. B. Schougaard, *Angewandte Chemie-International Edition*, 2011, **50**, 6884-6887.

12. G. Wang, H. Liu, J. Liu, S. Qiao, G. M. Lu, P. Munroe and H. Ahn, *Advanced Materials*, 2010, **22**, 4944-4948.

13. S. W. Oh, S. T. Myung, S. M. Oh, K. H. Oh, K. Amine, B. Scrosati and Y. K. Sun, *Advanced Materials*, 2010, **22**, 4842-+.

14. X.-Z. Liao, Z.-F. Ma, Q. Gong, Y.-S. He, L. Pei and L.-J. Zeng, *Electrochem. Commun.*, 2008, **10**, 691-694.

15. S. S. Zhang, K. Xu and T. R. Jow, *J. Power Sources*, 2006, **159**, 702-707.

16. A. L. Bard , L. R. Faulkner , *Electrochemical Methods* , 2nd ed. , Wiley ,**2001** .